JOC Article

Regioselectivity and Nucleophilic Control in the Cyclopropane Ring Opening of Duocarmycin SA Derivatives under Neutral and Acid Conditions: A Quantum Mechanical Study in the Gas Phase and in Solution

Paola Cimino,[†,‡] Luigi Gomez-Paloma,[‡] and Vincenzo Barone*[,†]

Dipartimento di Chimica, Università Federico II, Complesso Universitario Monte S.Angelo, via Cintia, I-80126 Napoli, Italy, and Dipartimento di Scienze Farmaceutiche, Università di Salerno, via Ponte don Melillo, 84084, Fisciano (SA), Italy

baronev@unina.it

Received May 15, 2004

We present a quantum mechanical investigation of the nucleophilic addition to the cyclopropane ring of a representative member of antitumor antibiotics related to CC-1065. We have analyzed, in particular, the regioselectivity of the reaction and its tuning by the nature of the etheroatom (O or N) in the nucleophile under both neutral and acidic conditions. Our results are in agreement with the experimental trends and suggest that, contrary to methanol, N-bases can be effective also under neutral conditions, irrespective of the additional steric constraints experienced in the biologically active substrate (DNA). The reliability of the computational protocol, rooted in the density functional theory coupled to a refined continuum solvent model, allows us to put forward reliable structure/reactivity relationships and to interpret the results in terms of reactivity indexes (hardness, electrophilic character).

Introduction

Sequence-selective alkylation of duplex DNA is the key to the biological activity of antitumor antibiotics related to CC-1065, whose parent members are duocarmycin SA (DSA, Figure 1) and duocarmycin A (DA).[1−3] The DNA alkylation reaction proceeds by a reversible, stereoelectronically controlled adenine N3 nucleophilic addition to the least substituted carbon atom belonging to the cyclopropane ring of the antibiotic within AT-rich minor groove regions of duplex DNA.[1]

Several models have been put forth in an effort to explain the rate enhancement associated with DNA alkylation by DSA and its derivatives with respect to comparable processes in solution. First, the reactivity of these systems can be related to specific characteristics of the alkylating agents. Indeed, several experimental data have convincingly shown that the reaction of DSA derivatives with nucleophiles can be highly sensitive to modification of the electrophile structure[4−6] and to protonation of the carbonyl moiety.[7−10] Our previous quantum mechanical study[11] on the solvolysis reaction with methanol of DSA derivatives under acid conditions has pointed out structure−reactivity relationships in agreement with experimental studies.

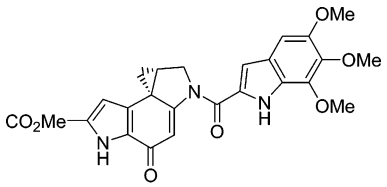

(+)-DSA

FIGURE 1. Structure of natural compound (+)-DSA.

On the other hand, it has been suggested that DNA would provide an enviroment specifically designed for activating the DSA structure and that the selectivity of DNA-alkylating agents would be the result of their preassociation with the biological substrate. Only indirect evidence has been given that the DNA alkylation se-

[†] Università Federico II.
[‡] Università di Salerno.

(1) Boger, D. L.; Johnson, D. L. *Angew. Chem., Int. Ed. Engl.* **1996**, *35*, 1438−1474.
(2) Boger, D. L.; Hertzog, D. L.; Bollinger B.; Johnson, D. L.; Cai H.; Goldberg, J.; Turnbull, P. *J. Am. Chem. Soc.* **1997**, *119*, 4977−4986.
(3) Boger, D. L.; Bollinger B.; Hertzog, D. L.; Johnson, D. L.; Cai H.; Mesini, P.; Garbaccio, R. M.; Jin, Q.; Kitos, P. A. *J. Am. Chem. Soc.* **1997**, *119*, 4987−4998.
(4) Baraldi, P. G.; Balboni, G.; Pavani, M. G.; Spalluto, G.; Tabrizi, M. A.; De Clercq, E.; Balzarini, J.; Bando, T.; Sugiyama, H.; Romagnoli, R. *J. Med. Chem.* **2001**, *44*, 2536−2543.
(5) Nagamura, S.; Asai, A.; Kobayashi, E.; Gomi, K.; Saito, H. *Bioorg. Med. Chem.* **1997**, *5*, 623−630.
(6) Amishiro, N.; Nagamura, S.; Kobayashi, E.; Okamoto, A.; Gomi, K.; Okabe, M.; Saito, H. *Bioorg. Med. Chem.* **2000**, *8*, 1637−1643.
(7) Boger, D. L.; Goldberg, J. A.; McKie, A. *Bioorg. Med. Chem. Lett.* **1996**, *6*, 1955−1960.
(8) Boger, D. L.; Santillan, A., Jr.; Searcey, M.; Jin, Q. *J. Org. Chem.* **1999**, *64*, 5241−5244.
(9) Boger, D. L.; Wysocki, R. J., Jr.; Ishizaki, T. *J. Am. Chem. Soc.* **1990**, *112*, 5230−5240.
(10) Boger, D. L.; Mesini, P. *J. Am. Chem. Soc.* **1994**, *116*, 11335−11348.
(11) Cimino, P.; Improta, R.; Bifulco, G.; Riccio, R.; Gomez-Paloma, L.; Barone, V. *J. Org. Chem.* **2004**, *69*, 2816−2824.

10.1021/jo049178k CCC: $27.50
Published on Web 09/29/2004

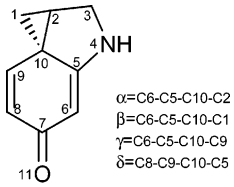

1

FIGURE 2. Structure of the model compound analyzed in this study.

quence selectivity could be induced by a conformational change[12] of the agent upon noncovalent binding to DNA, which in turn activates the agent toward nucleophilic attack.[13−15]

In summary, despite considerable experimental efforts, some key factors of the catalysis observed in the presence of DNA with respect to the reaction with small nucleophiles in solution are still unknown. First, the role that the nature of the nucleophilic species could have in the different observed rates has to be investigated. In fact, the nucleophile involved in the reaction in solution of DSA and its derivatives is methanol (or water), whereas an adenine plays the role of nucleophile in DNA.

Thus, the first part of the present contribution is devoted to analyze the different reactivity of typical nucleophiles, namely methanol, methylamine, and pyridine, toward a model alkylating agent (Figure 2) under both neutral and acid conditions by a quantum chemical approach employing a density functional method (PBE0)[16] coupled to a continuum solvent model (PCM).[17]

We have analyzed structure−reactivity relationships by comparing energetic, structural, and electronic parameters along the reaction paths of these prototypical systems. Next, we have tried to interpret the relative reactivity of the selected systems, in terms of hardness (η_{DA})[18] and electrophilicity (ω)[19] indexes, obtained by DFT calculations.

The second part of the study is devoted to an analogous investigation of the regioselectivity of the reaction and of the stereoelectronic factors by which it is influenced. Indeed, experimental studies on the reaction of several DSA analogues with methanol at low pH revealed a preferential attack to the least substituted carbon atom of the cyclopropyl ring (C1).[20] Here we will show that this selectivity may be interpreted in terms of local descriptors (Fukui fuction and regional softness).[21,22]

The most significant outcome of the present study is the inequivocal demonstration that, contrary to methanol, nitrogen nucleophiles can be effective also under neutral conditions. Thus, the overall picture sketched by our computations is in full agreement with experimental evidence and strongly suggests that, together with the steric factors invoked in previous qualitative models, electronic effects cannot be neglected for a satisfactory mechanistic explanation of sequence-selective alkylation in duplex DNA.

Methods

Computational Details. All of the calculations were carried out using the Gaussian03 package.[23] In the gas phase, all structures were fully optimized and characterized as minima or transition states by calculating the harmonic vibrational frequencies at the PBE0/6-31G(d) level.[16] At these geometries, single-point energy evaluations were done at PBE0/6-31G(d,p), PBE0/6-31+G(d,p), PBE0/6-311+G(d,p), and PBE0/6-311+G(2d,2p) levels.[24] Zero-point energies (ZPEs) and thermal contributions to thermodynamic functions and activation parameters were computed from PBE0/6-31G(d) structures and harmonic frequencies by using the rigid rotor/harmonic oscillator approximation and the standard expressions for an ideal gas in the canonical ensemble at 298.15 K and 1 atm.

Solvent effects have been taken into account by the self-consistent reaction field (SCRF) method using the so-called polarizable continuum model (PCM),[17] in which the solvent is represented by an infinite dielectric medium characterized by the relative dielectric constant of the bulk. We recall that the solvation energies issuing from PCM computations have the status of free energies, since they take implicitly into account thermal and entropic contributions of the solvent.[25] Harmonic frequencies computed in the gas-phase were used to evaluate the corresponding contributions of the solute.

The whole path for each reaction was traced by using the intrinsic reaction coordinate (IRC) at the PBE0/6-31G (d) level. The IRC calculation started from the optimized transition structure and followed the reaction path in both directions, toward the two minima it connects. We used up to 10 steps in each direction, with a step size of 0.3 amu$^{-1/2}$ bohr. Despite its limitations, the IRC[26] provides a very convenient description of reaction mechanisms as they are qualitatively treated by organic chemists.

The electronic structures were then analyzed by the natural bond orbital (NBO) model which allows us to evaluate the

(12) Boger, D. L.; Santillan, A., Jr.; Searcey, M.; Jin, Q. *J. Am. Chem. Soc.* **1998**, *120*, 11554−11557.
(13) Boger, D. L.; Garbaccio, R. M. *J. Org. Chem.* **1999**, *64*, 5666−5669.
(14) Boger, D. L.; Boyce, C. W.; Johnson, D. L. *Bioorg. Med. Chem. Lett.* **1997**, *7*, 233−238.
(15) Ambroise, Y.; Boger, D. L. *Bioorg. Med. Chem. Lett.* **2002**, *12*, 303−306.
(16) Adamo, C.; Barone, V. *J. Chem. Phys.* **1999**, *110*, 6158−6170.
(17) Cossi, M.; Rega, N.; Scalmani, G.; Barone, V. *J. Chem. Phys.* **2002**, *117*, 43−54.
(18) Ciofini, I.; Hazebroucq, S.; Joubert, L.; Adamo, C. *Theor. Chem. Acc.* **2004**, *111*, 188−195.
(19) Parr, R. G.; Szentpaly, L.; Liu, S. *J. Am. Chem. Soc.* **1999**, *121*, 1922−1924.
(20) Boger, D. L.; Goldberg, J.; McKie, J. A. *Bioorg. Med. Chem. Lett.* **1996**, *6*, 1955−1960.
(21) Roy, R. K.; Pal, S.; Hirao, K. *J. Phys. Chem.* **1999**, *110*, 8236−8245.
(22) Roy, R. K.; Hirao, K.; Pal, S. *J. Phys. Chem.* **2000**, *113*, 1372−1379.
(23) Gaussian 03, Revision B.4: Frisch, M. J.; Trucks, G. W.; Schlegel, H. B.; Scuseria, G. E.; Robb, M. A.; Cheeseman, J. R.; Montgomery, J. A., Jr.; Vreven, T.; Kudin, K. N.; Burant, J. C.; Millam, J. M.; Iyengar, S. S.; Tomasi, J.; Barone, V.; Mennucci, B.; Cossi, M.; Scalmani, G.; Rega, N.; Petersson, G. A.; Nakatsuji, H.; Hada, M.; Ehara, M.; Toyota, K.; Fukuda, R.; Hasegawa, J.; Ishida, M.; Nakajima, T.; Honda, Y.; Kitao, O.; Nakai, H.; Klene, M.; Li, X.; Knox, J. E.; Hratchian, H. P.; Cross, J. B.; Adamo, C.; Jaramillo, J.; Gomperts, R.; Stratmann, R. E.; Yazyev, O.; Austin, A. J.; Cammi, R.; Pomelli, C.; Ochterski, J. W.; Ayala, P. Y.; Morokuma, K.; Voth, G. A.; Salvador, P.; Dannenberg, J. J.; Zakrewski, V. G.; Dapprich, S.; Daniels, A. D.; Strain, M. C.; Farkas, O.; Malick, D. K.; Rabuck, A. D.; Raghavachari, K.; Foresman, J. B.; Ortiz, J. V.; Cui, Q.; Baboul, A. G.; Clifford, S.; Cioslowski, J.; Stefanov, B. B.; Liu, G.; Liashenko, A.; Piskorz, P.; Komaromi, I.; Martin, R. L.; Fox, D. J.; Keith, T.; Al-Laham, M. A.; Peng, C. Y.; Nanayakkara, A.; Challacombe, M.; Gill, P. M. W.; Johnson, B.; Chen, W.; Wong, M. W.; Gonzalez, C.; Pople, J. A. Gaussian, Inc., Pittsburgh, PA, 2003.
(24) A description of basis sets and standard computational methods can be found in: Foresman, J. B.; Frisch, A. E. *Exploring Chemistry with Electronic Structure Methods*, 2nd ed.; Gaussian Inc., Pittsburgh, PA, 1996.
(25) Tomasi, J.; Persico, M. *Chem. Rev.* **1994**, *94*, 2027.
(26) Gonzalez, C.; Schlegel, H. B. *J. Phys. Chem.* **1990**, *16*, 1170−1176.

stabilization energy connected to interactions between occupied orbitals of one reactant and empty orbitals of the second one.[27]

Reactivity Indexes. In recent years, reactivity descriptors such as hardness, softness, Fukui function, etc. have emerged as powerful tools in predicting both the overall reactivity and the site selectivity of a molecule.

We have selected as global descriptors the electrophilicity ω (intramolecular parameter that depends only on the electronic characteristics of the acceptor species) and the donor−acceptor hardness η_{DA} (intermolecular parameter).

The ω index quantifies the tendency of a molecule to "soak up" electrons, so that a high value corresponds to a great ability of the system to attract electrons from a generic donor molecule. On the other hand small values of the hardness η_{DA} indicate a strong interaction between donor and acceptor species, since this corresponds to a small energy gap between the donor HOMO and the acceptor LUMO.

The hardness has been defined[28−30] as the difference between the vertical ionization energy (I) and electron affinity (A) of the neutral molecule, $\eta = I - A$ where $I = E(N = N_0 - 1) - E(N = N_0)$ and $A = E(N = N_0) - E(N = N_0 + 1)$, N_0 being the number of electrons in the ground state of the system. This requires the calculation of the energies of the neutral (N_0 electron system), cationic ($N_0 - 1$ electron system), and anionic ($N_0 + 1$ electron system) forms of each system. The electronegativity (χ) and the electronic chemical potential (μ) have been defined as $\chi = (I + A)/2 = -\mu$. The definition of electrophilicity index (ω), given by Parr and co-workers,[19] is $\omega = \mu^2/2\eta$. Finally, the donor−acceptor intermolecular hardness (η_{DA}) is $\eta_{DA} = (I_D - A_A)$, where A_A is the electron affinity of the acceptor A and I_D the vertical ionization energy of the donor molecule D.[18]

We have used also the local softness s_k^+ and s_k^- and Fukui function f_k^+ and f_k^- for determining the site selectivity of the substrate upon the nucleophilic attack.[21,22] The s_k^+ and s_k^- indexes are suited for studies of nucleophilic and electrophilic attack, respectively. Moreover, the prediction of the most reactive site has been done also by using the so-called relative electrophilicity, s_k^+/s_k^-. The local softness $s(r)$ has been defined as: $s(r) = (\delta\rho\ (r)/\delta\mu)_{v(r)}$ where $\rho(r)$ is the electron density at the site r and $v(r)$ is the so-called external potential.

The local softness $s(r)$ can be rewritten as: $s(r) = f(r)S$, where $f(r)$ is the so-called Fukui function and S is the global softness. Then, $f(r)$ is defined as $f(r) = (\delta\rho(r)/\delta N)$, where N is the number of electrons of the chemical species and S is defined as $S = 1/(I - A)$. In a finite-difference approximation, the f_k values are calculated as $f_k^+ = q_k(N + 1) - q_k(N)$, for nucleophilic attack and $f_k^- = q_k(N) - q_k(N - 1)$, for electrophilic attack, where q_k is the gross electronic population of atom k in the molecule.

The f_k^+, f_k^-, s_k^+, and s_k^- values have been obtained at the PBE0/6-31G(d) level using Hirshfeld population analysis[31] recently implemented in the G03 package.

Results and Discussion

We have selected the DSA derivative **1**, shown in Figure 2, because it is the simplest compound containing all the structural elements able to tune the reactivity in a significant way, namely cyclopropane, cycloexadienone, and flanking nitrogen heterocycle. As a matter of fact, the first moiety is the reactive center, the second provides the driving force to the reaction in developing an aromatic system, and finally, the third moiety adds a key contribution to the unusual chemical stability of DSA. It was recognized that the simple spirocyclopropylcycloexadienone lacking this nitrogen is highly reactive. Removal of this nitrogen inhibits the ability to perform DNA alkylation.

SCHEME 1. Schematic Diagram of the Solvolysis Reaction

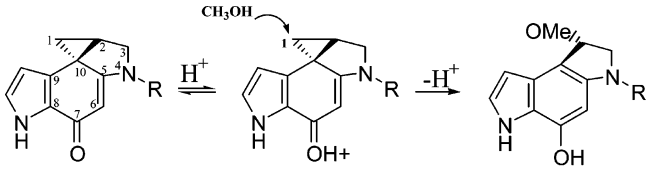

pH=3.O ⇒ 1. Rapid and reversible protonation
2. Slow nucleophylic attack (S_N2) on the least substitued cyclopropane carbon (C1)

Three different nucleophiles have been considered, CH_3OH, CH_3NH_2, and pyridine, since the first compound has been examined in experimental and computational studies in solution,[11] whereas a nitrogen nucleophile (adenine) performs the DNA alkylation. To separate the effects related to the nature of the attacking atom and to its hybridization state, we have considered both methylamine, in which the nitrogen atom has the same sp^3 hybridization as the methanol oxygen, and pyridine, whose nitrogen has the same sp^2 hybridization as adenine N3. We hope in this way to obtain an unbiased evaluation of electronic effects, before taking into account the steric effects, which are surely also operative in DNA.

Several experimental studies have shown that the neutral form of the ligand is bound to the DNA site, whereas the solvolysis of DSA with methanol proceeds only under acid conditions (i.e., involves a protonated DSA, Scheme 1).[32] Thus, we decided to investigate the attack of prototypical nucleophiles to both the neutral (**1**) and protonated (**1p**) forms of our model compound in the gas phase and in aqueous solution.

In all cases, we have evaluated the bare energy barriers $\Delta E^{\ddagger}$ (i.e., the electronic energy differences between TS's and the corresponding reactants), together with the corresponding free energies ($\Delta G^{\ddagger}$) which include zero-point, thermal, and entropic contributions (collectively referred to as nonpotential energy, NPE, terms). Table 1 shows that $\Delta E^{\ddagger}$'s and $\Delta G^{\ddagger}$ have parallel trends: as a consequence the results will be presented in terms of free energies, which have a closer correspondence with experimental data, but the interpretation will be based on electronic contributions only.

Basis set extension introduces systematic modifications in the results but does not change general trends (Figure 3). As a consequence, in the following we will make explicit reference to PBE0/6-31G(d) results only.

Nucleophilic Effects. Acid Conditions. We start with a comparative analysis of the ring-opening of compound **1** in its protonated form (**1p**) by nucleophilic attack of methanol (reference system), methylamine, and pyridine at the least substituted carbon atom (C1) in the

(27) Reed, A. E.; Curtiss, L. A.; Weinhold, F. *Chem. Rev.* **1988**, *88*, 899−926.
(28) Chermette, H. *J. Comput. Chem.* **1999**, *20*, 129−154.
(29) Parr, R.; Pearson, R. G. *J. Am. Chem. Soc.* **1983**, *105*, 7512−7516.
(30) Pearson, R. G. *Chemical Hardness*; VCH: Weinheim, 1997.
(31) Hirshfeld, F. L. *Theor. Chim. Acta* **1977**, *44*, 129−131.
(32) Warpehoski, M. A.; Harper, D. E. *J. Am. Chem. Soc.* **1994**, *116*, 7573−7580.

TABLE 1. Energy ($\Delta E^{\ddagger}$ and ΔE) and Free Energy ($\Delta G^{\ddagger}$ and ΔG at 298.15 K, 1 atm) Differences in the Gas Phase (PBEO/6-31G(d)) and in Aqueous Solution (PCM PBE0/6-31G(d)) for Compounds 1 and 1p

nucleophile	TS reactants	1	1p	product−reactants	1	1p
gas phase (PBE0/6-31G (d))						
CH_3OH	$\Delta E^{\ddagger}$ (kcal/mol)	50.3	9.3	ΔE (kcal/mol)		−5.5
pyridine	$\Delta E^{\ddagger}$ (kcal/mol)	30.9	−0.8	ΔE (kcal/mol)	16.2	−31.5
CH_3NH_2	$\Delta E^{\ddagger}$ (kcal/mol)	29.7	−1.0	ΔE (kcal/mol)	26.6	−27.7
CH_3OH	$\Delta G^{\ddagger}$ (kcal/mol)	62.8	20.6	ΔG (kcal/mol)		18.9
pyridine	$\Delta G^{\ddagger}$ (kcal/mol)	42.4	9.9	ΔG (kcal/mol)	29.6	−17.0
CH_3NH_2	$\Delta G^{\ddagger}$ (kcal/mol)	41.7	9.8	ΔG (kcal/mol)	40.6	−12.7
aqueous solution (PCM-PBE0/6-31G (d))						
CH_3OH	$\Delta G^{\ddagger}$ (kcal/mol)	40.6	24.5	ΔG (kcal/mol)	35.5	23.9
pyridine	$\Delta G^{\ddagger}$ (kcal/mol)	33.4	20.1	ΔG (kcal/mol)	8.6	−13.5
CH_3NH_2	$\Delta G^{\ddagger}$ (kcal/mol)	28.3	16.2	ΔG (kcal/mol)	2.8	−19.3

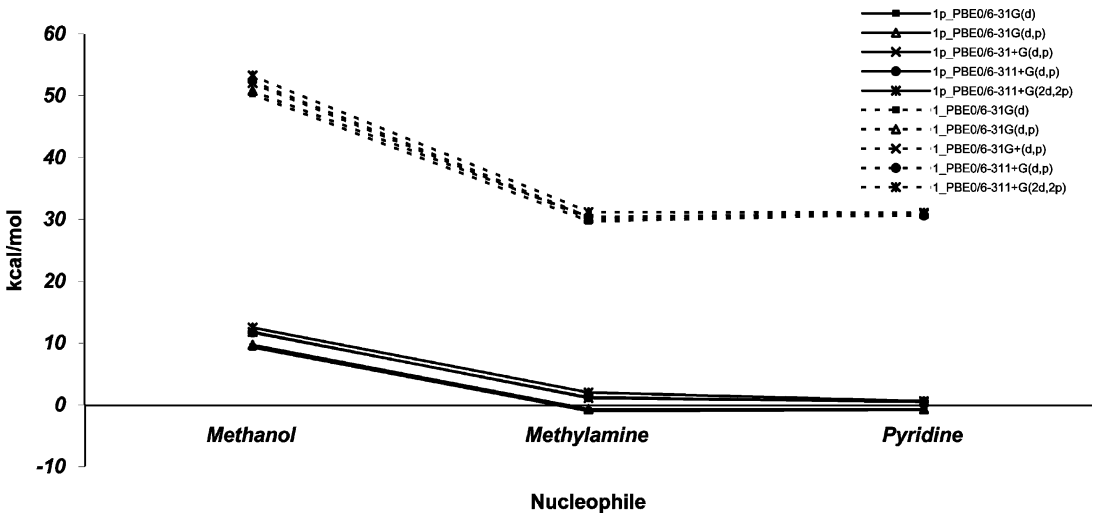

FIGURE 3. $\Delta E^{\ddagger}$ for the reactions of compounds **1** (dashed lines) and **1p** (full lines) with methanol, methylamine, and pyridine in the gas phase. See the text for details.

SCHEME 2. Schematic Pathway for the Acid-catalyzed S_N2 Reaction

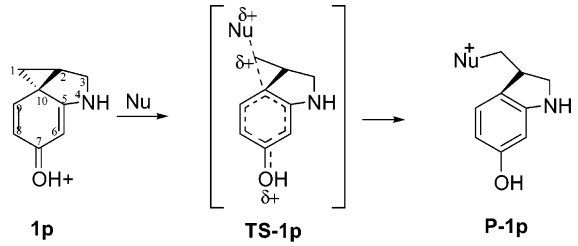

gas phase and in aqueous solution. The choice of carrying out these mechanistic studies in aqueous solution at neutral pH is due to the similarity between these conditions and the physiological medium in which the DNA alkylating reaction occurs.

Our results show that the acid-catalyzed reaction of compound **1** (**1p**) with methylamine and pyridine follows the same S_N2 mechanism predicted with methanol (Scheme 2). Examination of the calculated energies of the products relative to the reactants reveals that in the gas phase the reaction with CH_3NH_2 and pyridine is energetically favored over that with CH_3OH (Table 1). Indeed, the process is exothermic with both the nitrogen nucleophiles ($\Delta G = -12.7$ and -17.0 kcal/mol, respectively), whereas it is significantly endothermic with CH_3OH ($\Delta G = 18.9$ kcal/mol). It is noteworthy in this connection that entropy effects play a negligible role since ΔG and ΔH have closely parallel trends (Tables SI-1 and SI-2, Supporting Information). Moreover, the reaction of **1p** with methylamine and pyridine is governed by a free energy barrier about 10 kcal/mol lower than that with methanol ($\Delta G^{\ddagger} = 9.8$ and 9.9 kcal/mol vs. 20.6 kcal/mol with CH_3OH). These data are in agreement with the greater nucleophilicity of nitrogen with respect to oxygen.

The optimized geometrical structure of the stationary points governing the reactions under study (Table SI-3) shows that all of the products are characterized by a C1−C10 bond nearly coplanar to the ring (Figure 4). On the other hand, in the reactant **1p** the dienone moiety shows a significant out-of-plane distortion, and the cyclopropane ring is locked into an orientation that prevents a perpendicular arrangment (Figure 4). As shown in a previous study, the driving force of this transformation is the aromaticity.[11]

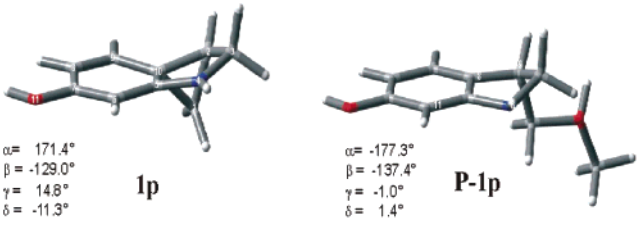

FIGURE 4. Structure of **1p** and **P-1p** optimized in the gas-phase (PBE0/6-31G(d)).

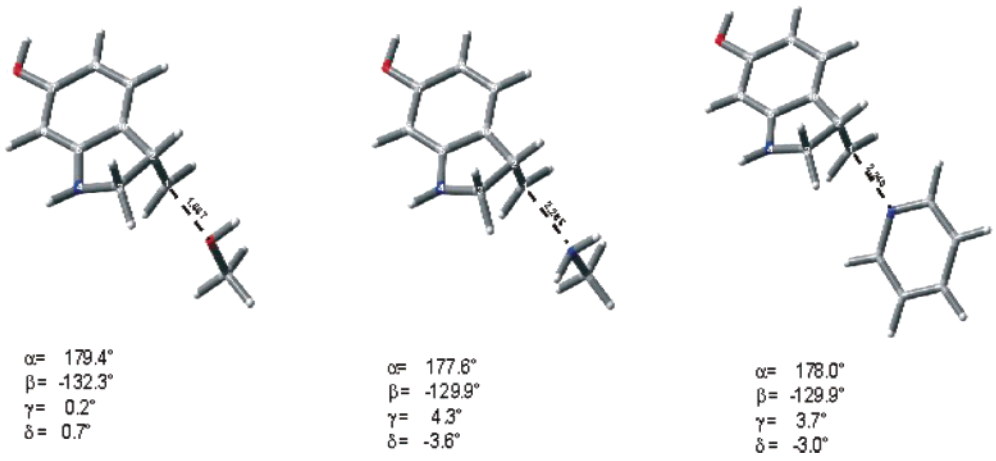

FIGURE 5. Transition-state structures of **1p** with methanol, methylamine, and pyridine in the gas phase (PBE0/6-31G(d)). The bond lengths are in angstroms.

TABLE 2. Bond Lengths for the TS-1 and TS-1p Structures Optimized in the Gas Phase and in Aqueous Solution (PBEO/6-31G(d))

		structure (attack on C1)	
	nucleophile	**1**	**1p**
gas phase (PBE0/6-31G (d))			
C1−C10 (Å)	CH_3OH	2.287	2.077
	pyridine	2.092	1.870
	CH_3NH_2	2.155	1.854
C10−Nu (Å)	CH_3OH	1.840	1.887
	pyridine	1.899	2.240
	CH_3NH_2	1.856	2.285
aqueous solution (PCM-PBE0/6-31G (d))			
C1−C10 (Å)	CH_3OH	2.126	1.192
	pyridine	1.970	1.872
	CH_3NH_2	1.926	1.818
C10−Nu (Å)	CH_3OH	1.834	2.009
	pyridine	2.082	2.230
	CH_3NH_2	2.162	2.325

TABLE 3. Natural Hybrid Orbitals for the TS-1p Structures with CH_3OH, CH_3NH_2, and Pyridine

nucleophile	bond	center	% natural hybrid p character
CH_3OH	C1C2(σ)	C1	63.3 ($sp^{1.72}$)
	C1C2(σ)	C2	75.4 ($sp^{3.06}$)
	C2C10(σ)	C10	70.9 ($sp^{2.44}$)
	C2C10(σ)	C2	78.0 ($sp^{3.55}$)
	LP*	C1	99.7 ($sp^{99.99}$ $d^{0.07}$)
	LP	C10	98.9 ($sp^{88.28}$)
CH_3NH_2	C1C2(σ)	C1	66.8 ($sp^{2.02}$)
	C1C2(σ)	C2	75.1 ($sp^{3.02}$)
	C2C10(σ)	C10	74.3 ($sp^{2.89}$)
	C2C10(σ)	C2	80.0 ($sp^{4.00}$)
	LP*	C1	98.1 ($sp^{52.62}$ $d^{0.03}$)
	LP	C10	93.9 ($sp^{15.33}$)
pyridine	C1C2(σ)	C1	65.2 ($sp^{1.87}$)
	C1C2(σ)	C2	75.1 ($sp^{3.03}$)
	C2C10(σ)	C10	72.9 ($sp^{2.68}$)
	C2C10(σ)	C2	79.8 ($sp^{3.97}$)
	C1C10(σ)	C1	97.0 ($sp^{33.14}d^{0.03}$)
	C1C10(σ)	C10	79.8 ($sp^{23.19}d^{0.01}$)

As is well-known, the Hammond postulate states that the properties of the TS are intermediate between reactants and products and are related to the position of the TS along the reaction coordinate. Thus, we can expect a "late" transition state with a structure close to that of the product for the reaction with methanol (Figure 5, Table SI-4 (Supporting Information)).

Indeed, in this TS the C1−O_{Me} bond is almost completely formed (1.887 Å vs. 1.537 Å in the product, Table 2), the C1−C10 distance is lengthened (2.077 vs. 1.554 Å) compared to that in the reactant **1p**, and at the same time, in the dienone ring the bonds C5−C6 (1.390 vs. 1.385 Å), C6−C7 (1.390 vs. 1.400 Å), C7−C8 (1.443 vs. 1.412 Å), C8−C9 (1.351 vs. 1.381 Å), C9−C10 (1.448 vs. 1.398 Å), and C10−C5 (1.463 vs. 1.419 Å) are changed, mirroring the developing aromaticity. Furthermore, the C2−C10 bond tends to become coplanar to the ring, while the C1−C10 bond shifts toward a more perpendicular arrangement. The dihedral angles (α = 179.4°, β = −132.3°, γ = 0.2°, δ = 0.7°) are indicative of a developing planarity of the dienone ring in the TS, whereas in **1p** this moiety is more distorted (α = 171.4°, β = −129.0°, γ = 14.8°, δ = −11.3°).

In agreement with the Hammond postulate, the transition state with methylamine resembles reactants (see Table SI-4 (Supporting Information), Figure 5). The C1−nucleophile bond in TS−CH_3NH_2 (2.285 Å) is not much developed relative to the bond in the product (1.512 Å) and the dienone moiety is more distorted than in TS−CH_3OH (α = 177.6° vs. 179.4°, β = −129.9° vs. −132.3°, γ = 4.3° vs. 0.2°, δ = −3.6° vs. 0.7°). The increase of the CH_3NH_2−C1 (2.285 Å) distance with respect to CH_3OH−C1 (1.887 Å) is an answer to the greater facility of CH_3NH_2 to react, whereas the distortion of the planar conformation of the dienone reflects a structure closer to the reactant than to the product. In particular, the hybridization of the C10 atom is still intermediate between sp^3 and sp^2 (Table 3) and this deviation from sp^2 arrangement is an indication of the lower conjugation in the dienone ring.

A comparative NBO analysis between the TSs (with CH_3OH and CH_3NH_2) reveals significant stabilizing interactions (Table 4) governing this reaction. This concerns, in particular, the interaction between the σ(C2−C10) bond and the p-type orbital, which develops at the C1 carbon (σ(C2−C10) to LP* (C1) = 23.4 and 37.9 kcal/mol with CH_3OH and CH_3NH_2, respectively), between the σ(C2−C10) bond and the p-type orbital on the C10 carbon atom (σ(C2−C10) to LP (C1) = 5.0 and 13.3 kcal/mol with CH_3OH and CH_3NH_2, respectively), and

TABLE 4. Stabilization Energies (E(2)) for the TS-1p Structures with CH_3OH, CH_3NH_2, and Pyridine

nucleophile	donor−acceptor	*E*(2) (kcal/mol)
CH_3OH	sp_{C1C2} to LP^*_{C1}	1.1
	sp_{C2C10} to LP^*_{C1}	23.4
	sp_{C2C10} to LP_{C10}	5.0
	sp_{C1C2} to LP_{C10}	10.8
CH_3NH_2	sp_{C1C2} to LP^*_{C1}	9.3
	sp_{C2C10} to LP^*_{C1}	37.9
	sp_{C2C10} to LP_{C10}	13.3
	sp_{C1C2} to LP_{C10}	22.0
pyridine	sp_{C2C10} to σ^*_{C1C10}	5.5
	sp_{C2C10} to σ^*_{C1C2}	2.0
	LP_{Nu} to σ^*_{C1C10}	22.7
	sp_{C1C2} to LP_{C10}	−
	sp_{C1C2} to σ^*_{C1C10}	2.5

between the σ(C1−C2) bond and the p-type orbital on C10 (σ(C1−C2) to LP (C1) = 10.8 and 22.0 kcal/mol with CH_3OH and CH_3NH_2, respectively).

These data confirm that the nonbonding nitrogen lone pair of methylamine is able to stabilize a transition state with a structure quite close to that of the reactant, with a consequent lower activation energy.

Let us now try to explain the effect on the reaction of the different hybridization state of nitrogen in CH_3NH_2 and pyridine. As seen before, the activation energy calculated for the reaction between **1p** and pyridine is the same as that predicted with CH_3NH_2 (9.8 kcal/mol), and the process is even more exothermic ($\Delta G = -17.0$ vs. −12.7 kcal/mol). In analogy with TS−CH_3NH_2, TS-pyridine (Figure 5, Table SI-4) also presents a quite long C1−nitrogen distance (2.240 vs. 1.481 Å in the product), a distortion of the dienone ring ($\alpha = 178.0°$, $\beta = -129.9°$, $\gamma = 3.7°$, $\delta = -3.0°$) and the *p*-character of C1 (Table 3), which are indicative of a TS structure quite close to that of the reactant. The most important electronic interaction in the transition state with pyridine involves the cyclopropyl C1−C10 bond (σ) and the LP* orbital of the pyridine nitrogen (22.7 kcal/mol). Thus, the stabilizing interactions operative for sp^2 and sp^3 nitrogen are not the same, despite of the very similar overall effect.

In conclusion, the barrier height in the process with CH_3OH is largely due to the energetic requirement for the development of a planar arrangment in TS compared to the significantly distorted configurations of methylamine and pyridine TSs. A comparison among the deformed structures characterizing the **1p** moiety in the TSs and the free ligand shows that the largest energy is required to reach the TS structure when the nucleophile is methanol (ΔE_{def} = 28.2, 13.9, and 13.0 kcal/mol for methanol, pyridine, and CH_3NH_2, respectively).

In aqueous solution, our computations predict that the barrier for the S_N2 reaction is significantly lower than in the gas phase (Table 1). Since in a previous work we have analyzed the systems in methanol,[11] we estimate the $\Delta G^{\ddagger}$ of the compound **1p** with CH_3OH and CH_3NH_2 also in methanol. The activation free energies computed in both solvents are very close ($\Delta G^{\ddagger}$ = 24.6 kcal/mol in methanol and $\Delta G^{\ddagger}$ = 24.5 kcal/mol in water with CH_3OH; $\Delta G^{\ddagger}$ = 16.1 kcal/mol in methanol and $\Delta G^{\ddagger}$ = 16.2 kcal/mol in water with CH_3NH_2). Thus, it appears that the change of reaction solvent does not affect the barrier energy for this reaction.

It is important to keep in mind that bulk solvent effects can be well represented by a structureless continuum model (here PCM),[17] whereas strong solute−solvent interactions require the explicit treatment of some water molecules at the QM level. This aspect is beyond the scope of the present work but will be properly dealt with in future studies devoted to a more quantitative evaluation of specific reaction rates.

From a geometrical point of view, our results show (Tables 2, SI-3 and SI-5 (Supporting Information)) that the solvent does not induce significant changes in the structures of reactants, transition states, and products.

In solution, the reaction with methanol is endothermic, whereas that with nitrogen nucleophiles is exothermic (ΔG is 23.9, −13.5, and −19.3 kcal/mol, respectively, with CH_3OH, pyridine, and CH_3NH_2), and the relative reactivity order of the nitrogen nucleophiles is reversed in favor of methylamine. In aqueous solution, the activation free energies for the reaction with CH_3OH, CH_3NH_2, and pyridine are increased, respectively, by 3.9, 10.2, and 6.4 kcal/mol by the presence of water. The dipole moments in the gas phase suggest that both the products and the transition structures with CH_3NH_2 (μ = 12.4 D and μ = 3.99 D) would be more highly solvated by polar solvents than their counterparts with pyridine (μ = 10.5 D and μ = 1.3 D). This results in an activation barrier in water for TS-pyr that is increased with respect to the gas-phase process by 6.4 kcal/mol, instead of the 10.2 kcal/mol found for TS-CH_3NH_2. An analogous trend is observed for the products.

In short, the computed free energy barrier with CH_3OH is higher than with CH_3NH_2 and with pyridine, both in gas phase and in solution.

It is finally noteworthy that the donor−acceptor intermolecular hardness η_{DA} correctly predicts the higher nucleophilicity of CH_3NH_2 and pyridine (η_{DA} = 6.18 eV with CH_3OH, η_{DA} = 4.98 eV with CH_3NH_2, η_{DA} = 4.94 eV with pyridine in gas-phase).

Neutral Conditions. In the next step of our analysis, we have investigated the mechanism of S_N2 reaction under neutral conditions (Scheme 3).

SCHEME 3. Schematic Pathway for the S_N2 Reaction under Neutral Conditions

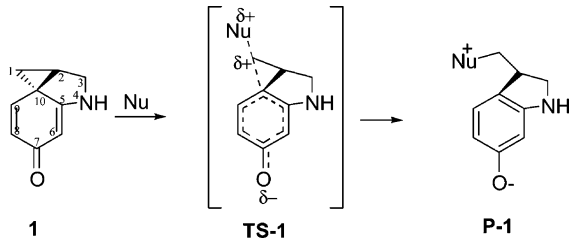

We recall that[11] protonation of the dienone oxygen atom leads to an increase of the aromatic character of the dienone and to a delocalization of the positive charge within the whole molecule (**1p**). The former effect leads to a weakening of the C1−C10 bond, whereas the latter effect increases the electrophilic character of the cyclopropyl carbon atoms (Table 5). Thus, both effects favor the nucleophilic substitution. As a consequence, **1p** is more reactive than **1** toward the nucleophilic substitution.

TABLE 5. Mulliken and NBO Charges for Compounds 1 and 1p Optimized in the Gas Phase and in Water Solution (PBEO/6-31G(d))

		structure	
		1	**1p**
gas phase			
Mulliken Charge (q) on CH_2 group	C1	0.061	0.158
Mulliken Charge (q) on CH group	C2	0.030	0.082
NBO Charge (q) on CH_2 group	C1	0.089	0.172
NBO Charge (q) on CH group	C2	0.025	0.078
aqueous solution			
Mulliken Charge (q) on CH_2 group	C1	0.078	0.139
Mulliken Charge (q) on CH group	C2	0.044	0.088
NBO Charge (q) on CH_2 group	C1	0.103	0.162
NBO Charge (q) on CH group	C2	0.051	0.084

The much higher ΔGs computed (Table 1) for the reaction on **1** in comparison to those on **1p** are indicative that the reaction in acid condition is favored with respect to that at neutral pH. We were unable to find the product (**P-1**) with methanol in the gas phase. Also the activation free energies ($\Delta G^{\ddagger}$ = 62.8 kcal/mol with CH_3OH, $\Delta G^{\ddagger}$ = 42.4 kcal/mol with pyridine and 41.7 kcal/mol with CH_3NH_2 in the gas phase) support this conclusion, confirming that the barriers for the neutral compound are higher than the corresponding values for the protonated molecule. Furthermore, the reaction is faster with CH_3NH_2 and with pyridine than with CH_3OH.

In the gas phase, the reaction with CH_3NH_2 and pyridine follows the same mechanism seen until now, whereas the reaction with methanol proceeds through a cyclic transition state (TS) involving a CH_3OH-N4 hydrogen bond (1.844 Å, Figure 6). However, the formation of that hydrogen bond involves a rotation of the CH_2 group around the C1−C2 bond with the consequent reduction of conjugative stabilization with respect to the protonated species. Since the developing aromaticity plays a dominant role in stabilizing the TS of the reaction involving **1p**, its reduction leads to a significant increase of the reaction barrier in the reaction involving **1** ($\Delta G^{\ddagger}$ = 20.6 and 62.8 kcal/mol for **1p**, and **1**, respectively).

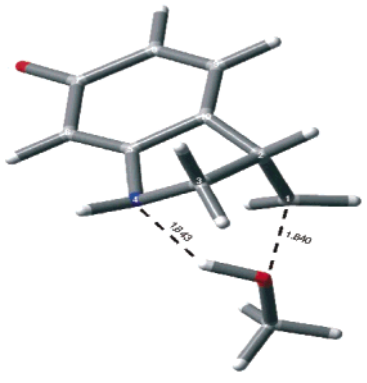

FIGURE 6. Transition-state structure for the reaction of **1** with methanol in the gas phase (PBE0/6-31G(d)). The bond lengths are in angstroms.

In aqueous solution, the reaction follows the same mechanism with all three nucleophiles. The effect of the solvent (water) on the reactivity can be evaluated by the reduction of both ΔG and $\Delta G^{\ddagger}$ (by about 10−20 kcal/mol) with respect to the corresponding reactions in the gas phase (Table 1). The computed bond lengths and dihedral angles (Table SI-4, Supporting Information) reveal in the transition states a developing benzylic-type conjugation close to that of the protonated forms. Moreover, the relative stabilization by a polar solvent (water) is effective only for neutral forms, as shown in Table 6 ($\Delta\Delta G^{\ddagger} = \Delta G^{\ddagger}_{aq} - \Delta G^{\ddagger}_{gas\ phase}$).

TABLE 6. $\Delta\Delta G^{\ddagger}$ in Aqueous Solution (PCM-PBEO/6-31G(d)) and the Gas Phase in (PBE0/6-31G(d)) for Compounds 1 and 1p

		structures			
		attack on C1		attack on C2	
	nucleophile	**1**	**1p**	**1**	**1p**
aqueous solution−gas phase					
$\Delta\Delta G^{\ddagger}$ (kcal/mol)	CH_3OH	−22.2	3.9	−22.6	3.3
$\Delta\Delta G^{\ddagger}$ (kcal/mol)	pyridine	−8.0	10.2	−7.8	9.8
$\Delta\Delta G^{\ddagger}$ (kcal/mol)	CH_3NH_2	−13.4	6.4	−13.3	6.3

The significant lowering of the activation barrier of **1** ($\Delta\Delta G^{\ddagger}$) in aqueous solution may be ascribed to an electrostatic stabilization. Indeed, the dipole moment variation between the protonated transition state (μ = 4.4 D with CH_3OH, μ = 3.99 D with CH_3NH_2 and μ = 1.3 D with pyridine in vacuo) and the reactant (μ = 1.3 D) is significantly lower than that of the neutral species (μ = 19.7 D with CH_3OH, μ = 17.5 D with CH_3NH_2 and μ = 16.0 D with pyridine in vacuo; μ = 6.6 D for the reactant). These data suggest that the unprotonated transition structure would be better solvated by polar solvents.

Analogous considerations can explain the greater stability of products with respect to reactants (with both nitrogen nucleophiles the process is exothermic) in solution. So, the dipole moments of the neutral products are 21.9 and 16.3 D, respectively, with CH_3NH_2 and pyridine and those of the protonated forms are 12.4 and 10.5 D.

In summary, our results indicate that the substitution reaction on neutral DSA derivatives does not proceed with CH_3OH, in agreement with experimental studies, whereas it is more probable with CH_3NH_2 and pyridine. Keeping in mind that the nucleophile involved in the DNA alkylation is an adenine nitrogen, whereas it is CH_3OH under solvolytic conditions, these data suggest that, at least, part of the rate enhancement in DNA is due to an intrisic nucleophilic effect.

The reactivity order of CH_3OH, CH_3NH_2, and pyridine toward **1** predicted by intermolecular hardnesses is in agreement with this hypothesis (i.e., 1p > 1; η_{DA} = 11.44 eV with CH_3OH and η_{DA} = 10.23 eV with CH_3NH_2 in the gas phase, η_{DA} = 10.20 eV with pyridine; ω of **1** is 0.7 eV and ω of **1p** is 4.4 eV in the gas phase). In particular, the trend for the nucleophiles is preserved (CH_3NH_2 > pyridine > CH_3OH), and a significant increase of η_{DA} is found in going from the protonated to the neutral system.

Regioselectivity. Experimental studies of the acid-catalyzed nucleophilic addition of CH_3OH to DSA derivatives established that solvolysis preferentially occurs with cleavage of the C1−C10 bond upon addition of a nucleophile to the least substituted C1 cyclopropane carbon versus cleavage of the C2−C10 bond with ring expansion and addition to C2 (Scheme 4).[20]

SCHEME 4. Acid-Catalyzed CH_3OH Addition (cat. CF_3SO_3H/CH_3OH, 25°C, 1 h, (93%))

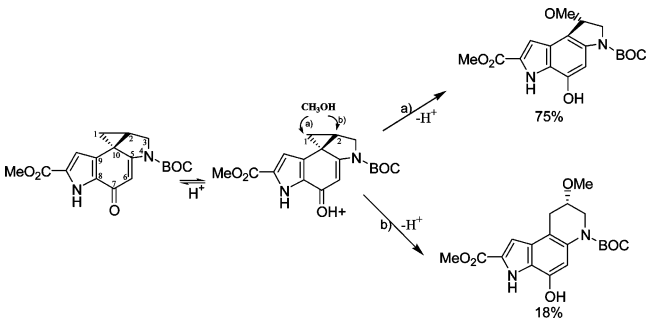

Thus, in the solvolytic reaction with methanol the DSA derivatives produce two types of compounds, which are due to the nucleophilic attack on the "less substituted" and "more substituted" carbon atom, respectively. Of course, the most abundant final product will depend on which of these two sites is more reactive toward the incoming reactant.

At the same time, DNA alkylation studies of several synthetic derivatives established that the regioselectivity of the DNA alkylation reaction is even greater than that of the solvolysis, leading exclusively to adenine N3 addition to the C1 cyclopropane atom.

Inspection of the TS governing the nucleophilic attack at C2 in acid conditions (Figure 7) shows that the reaction consists also in this case of a concerted single step, in which the bond-forming and -breaking processes occur almost simultaneously (Table SI-5).

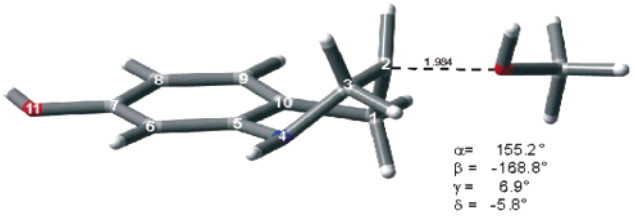

FIGURE 7. Transition-state structure of **1p** with methanol for the reaction with the nucleophilic attack on the carbon C2 (gas-phase, PBE0/6-31G(d)). The bond lengths are in angstroms.

A comparison of the activation free energies (Table 7) shows that $\Delta G^{\ddagger}$ for the first path (attack on C1) is lower than that for the second one (attack on C2). The energy values are: for **1p** in water $\Delta G^{\ddagger}$(C2) = 24.9 kcal/mol with CH_3OH, $\Delta G^{\ddagger}$(C2) = 22.2 kcal/mol with pyridine and $\Delta G^{\ddagger}$(C2) = 18.7 kcal/mol with CH_3NH_2 vs. $\Delta G^{\ddagger}$(C1) = 24.5 kcal/mol with CH_3OH, $\Delta G^{\ddagger}$(C1) = 20.1 kcal/mol with pyridine and $\Delta G^{\ddagger}$(C1) = 16.2 kcal/mol with CH_3NH_2.

This regioselectivity is related to the presence of a conjugated system allowing significant resonance stabilization and to the different electron-withdrawing ability of C1 and C2. For instance, the results collected in Table 5 show that for **1p** in aqueous solution the positive charge on the former carbon atom is significantly higher than on the latter atom according to both Mulliken and NBO population analysis.

Concerning nitrogen nucleophiles, a plausible reason for the preferred addition to C1 may be found in the energy difference between the deformed substrate in the two transition-states (for the reaction on C1: ΔE_{def} = 13.9 and 13.0 kcal/mol with pyridine and CH_3NH_2, respectively; for the reaction on C2: ΔE_{def} = 16.0 and 15.2 kcal/mol with pyridine and CH_3NH_2, respectively).

TABLE 7. Energy ($\Delta E^{\ddagger}$) and Free Energy ($\Delta G^{\ddagger}$ at 298.15 K, 1 atm) Barriers in the Gas Phase (PBEO/6-31G(d)) and in Aqueous Solution (PCM PBE0/6-31G(d)) for Compounds 1 and 1p

		structures			
		attack on C1		attack on C2	
	nucleophile	**1**	**1p**	**1**	**1p**
gas phase					
$\Delta E^{\ddagger}$ (kcal/mol)	CH_3OH	50.3	9.3	50.9	10.4
$\Delta E^{\ddagger}$ (kcal/mol)	pyridine	30.9	−0.8	32.4	1.7
$\Delta E^{\ddagger}$ (kcal/mol)	CH_3NH_2	29.7	−1.0	31.1	1.7
$\Delta G^{\ddagger}$ (kcal/mol)	CH_3OH	62.8	20.6	62.8	21.6
$\Delta G^{\ddagger}$ (kcal/mol)	pyridine	42.4	9.9	44.5	12.4
$\Delta G^{\ddagger}$ (kcal/mol)	CH_3NH_2	41.7	9.8	43.2	12.4
aqueous solution					
$\Delta G^{\ddagger}$ (kcal/mol)	CH_3OH	40.6	24.5	40.2	24.9
$\Delta G^{\ddagger}$ (kcal/mol)	pyridine	33.4	20.1	36.7	22.2
$\Delta G^{\ddagger}$ (kcal/mol)	CH_3NH_2	28.3	16.2	29.9	18.7

The different activation free energy for the two reaction channels is also indicative of the significant role played by the π electron interaction. When the interaction exists, the transition state is strongly stabilized, whereas in the deformed structure it is destabilized. In other words, when the dienone ring is in a planar conformation where the p-orbital of C10 is in conjugation with the π-system the reaction is faster (Figure 7, Table SI-5 (Supporting Information)).

In the transition state **1p** (C1), the C1−C10 bond adopts a conformation allowing maximum overlap between the p-orbital (C10) and π-orbitals, whereas in **1p** (C2) the C10 atom shifts down with a consequent loss in TS stabilization. The π-interactions in the transition state between the atoms of the dienone represent a major factor in this reaction and govern its rate.

Breaking the bond between C2 and C10 by the nucleophilic attack on C2 results in TS (C2) and the barrier energy increases (Table 7).

These data confirm that the acid reaction is regioselective, occurring with addition of a nucleophile to the least substituted cyclopropane carbon (C1), in agreement with experimental observations.

Coming next in the reaction in neutral conditions, the $\Delta G^{\ddagger}$'s computed (Table 7) for the two reaction channels are indicative that the reaction is even more regioselective. However, the slight increase of selectivity issuing from the data of Table 7 is not sufficient to explain the complete lack of any product of the attack on C2. This suggests that the regioselectivity of the adenine N3 alkylation reaction benefits not only from stereoelectronic control but also from specific steric effects.

Finally, we analyze the reactivity of the two centers (C1 and C2) in terms of local reactivity indexes (Table 8).

Although we are mainly concerned with qualitative trends, we have investigated the sensitivity of the results changes in the exchange-correlation functional and basis-set. The data collected in Table 8 point out the negligible effect of the functional and a number of other test computations show that this is also the case for the basis

TABLE 8. Condensed Fukui Functions (f^+ and f^-) and Atomic Softness Indexes (s^+ and s^-) of the Molecules Studied in This Work with Two Competitive Electrophilic Centers (Evaluated through Hirshfeld's Population Analysis Technique)

structure	atom	f^+	f^-	s^+	s^-	s^+/s^-	s^-/s^+
gas phase (PBE0/6-31G (d))							
PBE0/6-31G (d)							
1	C1	0.0528	0.0325	0.0083	0.0051	1.6254	0.6152
	C2	0.0393	0.0260	0.0062	0.0041	1.5128	0.6610
1p	C1	0.0598	0.0345	0.0074	0.0043	1.7352	0.5763
	C2	0.0408	0.0248	0.0050	0.0031	1.6446	0.6080
PBE/6-31G (d)							
1	C1	0.0534	0.0315	0.0064	0.0038	1.6254	0.6152
	C2	0.0395	0.0248	0.0047	0.0030	1.5128	0.6610
1p	C1	0.0590	0.0392	0.0073	0.0049	1.5041	0.6648
	C2	0.0403	0.0266	0.0050	0.0033	1.5187	0.6585
B3LYP/6-31G (d)							
1	C1	0.0527	0.0326	0.0061	0.0038	1.6185	0.6178
	C2	0.0393	0.0264	0.0045	0.0030	1.4997	0.6668
1p	C1	0.0597	0.0352	0.0073	0.0043	1.6966	0.5894
	C2	0.0408	0.0252	0.0050	0.0031	1.6201	0.6173
aqueous solution (PCM-PBE0/6-31G (d))							
1	C1	0.0551	0.0318	0.0067	0.0038	1.7313	0.5776
	C2	0.0393	0.0250	0.0048	0.0030	1.5739	0.6354
1p	C1	0.0584	0.0392	0.0073	0.0049	1.4883	0.6719
	C2	0.0400	0.0265	0.0050	0.0033	1.5101	0.662

set, except that unrealistic Hirshfeld charges are obtained upon addition of diffuse functions.

The two carbon atoms have comparable f_k^+, s_k^+ values and relative $f_k^+ > f_k^-$, $s_k^+ > s_k^-$: thus, they act as "electrophilic" centers. In molecule **1** and in its protonated form **1p**, both electrophilic local indexes (f_k^+, s_k^+) of C1 are larger than those of C2 (for **1**: $f_{C1}^+ = 0.0528$, $s_{C1}^+ = 0.00832$, $f_{C2}^+ = 0.0393$, $s_{C2}^+ = 0.00619$; for **1p**: $f_{C1}^+ = 0.0598$, $s_{C1}^+ = 0.00739$, $f_{C2}^+ = 0.0408$, $s_{C2}^+ = 0.00504$ in the gas phase). Hence, C1 should be the preferred site for a nucleophilic attack. Also the trend predicted by s_k^+/s_k^- values is in agreement with the experimental trend of site selectivity in all cases.

Concluding Remarks

The present paper reports the essential results of a comprehensive quantum mechanical study of the reaction between a model duocarmycin analogue **1** and some model nucleophiles (CH_3OH, CH_3NH_2, and pyridine) in the gas phase and in solution. The scenario sketched by our computations is fully consistent with the available experimental indications concerning both reactivity and regioselectivity.

The computed activation free energies point out that acid catalysis is mandatory for methanol, but neutral conditions could be sufficient for stronger nucleophiles such as methylamine and pyridine. Thus, together with steric interactions, intrinsic electronic effects could explain the different reactivity between methanol solution and the biologically active substrate.

The second part of the present study provides insights into the origin of the regioselectivity of the reaction (C1 > C2). Two important factors have been evidenced, namely the different electrofilicity of the two carbon atoms (C1 > C2), and the formation of a resonance stabilized system only for one of the competitive reaction channels (attack at C1).

From a methodological point of view, the present study confirms the usefulness of a theoretical investigation for the design of new and more effective compounds, highlighting the necessity of taking solvent effects in to the proper account. As a matter of fact, solute−solvent interactions play a dominant role both in increasing the reactivity of protonated forms and in discriminating between sp^3 and sp^2 nucleophiles. It is also noteworthy that qualitative considerations can be based on computed reactivity indexes (e.g., η and ω).

From a more general point of view, our results, besides providing deeper insight on the structure/reactivity relationships and on mechanistic aspects, pave the route for the study of the interaction between duocarmycins and DNA. Work is in progress in this connection in our laboratory.

Acknowledgment. We thank the Italian Ministry of University and Research (MIUR) and Gaussian Inc. for financial support.

Supporting Information Available: Tables SI-1, SI-2, SI-3, SI-4, and SI-5. This material is available free of charge via the Internet at http://pubs.acs.org.

JO049178K